

## Terahertz wave generation from gas plasma using a phase compensator with attosecond phase-control accuracy

Jianming Dai and X.-C. Zhang

Citation: *Appl. Phys. Lett.* **94**, 021117 (2009); doi: 10.1063/1.3068501

View online: <http://dx.doi.org/10.1063/1.3068501>

View Table of Contents: <http://apl.aip.org/resource/1/APPLAB/v94/i2>

Published by the [AIP Publishing LLC](#).

---

### Additional information on *Appl. Phys. Lett.*

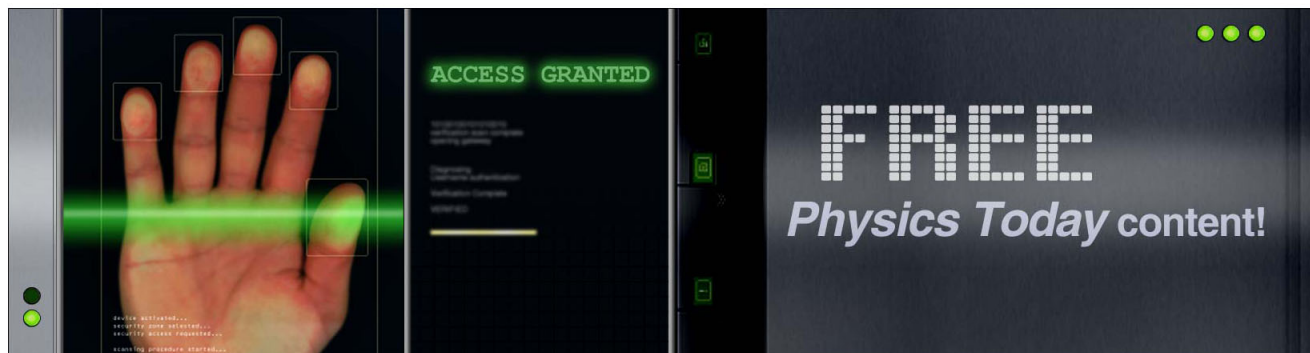
Journal Homepage: <http://apl.aip.org/>

Journal Information: [http://apl.aip.org/about/about\\_the\\_journal](http://apl.aip.org/about/about_the_journal)

Top downloads: [http://apl.aip.org/features/most\\_downloaded](http://apl.aip.org/features/most_downloaded)

Information for Authors: <http://apl.aip.org/authors>

## ADVERTISEMENT



# Terahertz wave generation from gas plasma using a phase compensator with attosecond phase-control accuracy

Jianming Dai and X.-C. Zhang<sup>a)</sup>

Center for Terahertz Research, Rensselaer Polytechnic Institute, Troy, New York 12180, USA

(Received 23 September 2008; accepted 17 December 2008; published online 15 January 2009)

We report the use of a precise phase compensator for the generation of intense terahertz waves from laser-induced gas plasma excited by a femtosecond pulse ( $\omega$ ) and its second harmonic ( $2\omega$ ) at both close contact and standoff distances. The attosecond accuracy phase-control capability of the device enables further optimization of the terahertz emission from gas plasma and elimination of the temporal walkoff between the  $\omega$  and  $2\omega$  pulses traveling in dispersive media, resulting in intense terahertz generation at a distance of over 100 m by sending the optical beams far away and focusing them locally. © 2009 American Institute of Physics. [DOI: 10.1063/1.3068501]

Recently, terahertz wave generation from laser-induced gas plasma with excitation by femtosecond pulses at both 800 nm ( $\omega$ ) and 400 nm ( $2\omega$ ) through nonlinear optical wave mixing has attracted greater attention due to the remarkable terahertz beam quality and directionality, bandwidth, terahertz electric field, as well as its potential applications in nonlinear terahertz spectroscopy and remote sensing and imaging.<sup>1–10</sup> However, the physical mechanism of the terahertz emission in gas plasma is still under debate. Up to now, there are essentially two models used to explain the nonlinear optical processes responsible for the terahertz generation in gas plasma, i.e., four-wave mixing model and asymmetric transient current model. Both of the models can partially explain the experimental results.<sup>1,6,11</sup> Nevertheless, both models indicate that the terahertz generation efficiency is highly dependent on the relative phase between  $\omega$  and  $2\omega$  pulses. Our previous experimental results proved that both the polarization of  $\omega$  and  $2\omega$  beams and the relative phase between  $\omega$  and  $2\omega$  pulses are very critical to the terahertz generation efficiency.<sup>11</sup> To more efficiently generate terahertz waves using gas plasma as the emitter, precise and stable controlling of the relative phase is very crucial. In this letter, we reported the use of a phase compensator for more efficient terahertz wave generation from gas plasma with attosecond phase-control accuracy. Furthermore, using this phase compensator we are able to generate stable, intense, broadband terahertz waves by sending the two optical pulses (800 and 400 nm pulses) far away and focusing them locally to create air plasma with the compensation of the temporal walkoff between the  $\omega$  and  $2\omega$  pulses induced by the dispersion in ambient air, which will find potential applications in terahertz remote sensing and imaging.

Our phase compensator is based on a typical interferometer, as shown inside the dashed line in Fig. 1. A femtosecond pulse at 800 nm generates its second harmonic pulse at 400 nm after passing through a type-I beta barium borate (BBO) crystal. The  $\omega$  and  $2\omega$  beams, which have their polarizations perpendicular to each other, are separated by a dichroic mirror (DM). A half waveplate (HWP) in the  $2\omega$  arm is used to rotate the polarization of the  $2\omega$  beam. In the  $\omega$  arm, instead of using a conventional retroreflector com-

pared with a translation stage to directly change the optical delay between the two arms, a fused silica wedge pair with a small wedge angle of  $2.8^\circ$  is used to finely control the delay. Finally, the  $\omega$  and  $2\omega$  beams are combined with the second DM. The advantage of using the wedge pair as the optical delay device over the conventional optical delay line is that the wedge pair can convert relatively coarser mechanical stage steps to very finer steps in optical delay through the relationship  $\Delta\tau = \Delta l(n-1)\tan(\theta)$ , where  $\Delta l$  is the step size of the mechanical translation stage,  $n$  is the refractive index of the fused silica at 800 nm in air,  $\theta$  is the wedge angle, and  $\Delta\tau$  is the resulting optical delay step. In our current setup, a  $0.5 \mu\text{m}$  step made by the mechanical translation stage is equivalent to an optical delay step of 11 nm, corresponding to about 37 as in time. Therefore, regular computer controlled stages can be used for fine optical delay. Meanwhile, the delay instability solely caused by the translation stages or even piezostages in conventional delay lines can be reduced by a factor of 90.

A 1 kHz Ti:sapphire amplified laser delivering about  $800 \mu\text{J}$ , 100 fs pulses with a central wavelength at 800 nm is used. After the phase compensator, the  $\omega$  and  $2\omega$  beams, after passing through a certain distance in the air, are focused by an aluminum coated parabolic mirror to create plasma, as shown in Fig. 1. The total laser energy after the parabolic is about  $500 \mu\text{J}$ , which corresponds to a throughput of about 62%. The terahertz waves generated from the plasma are

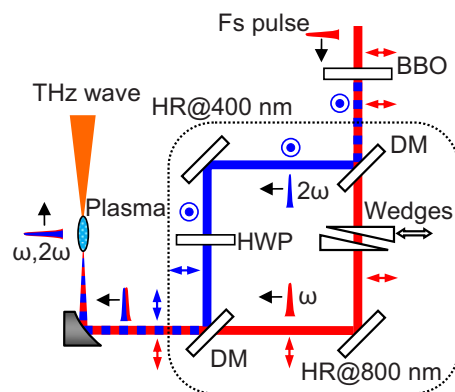


FIG. 1. (Color online) Schematic of the phase compensator incorporated with a wedge pair: DM used to separate or recombine  $\omega$  and  $2\omega$  beams; HWP used to control the polarization of the  $2\omega$  beam.

<sup>a)</sup>Electronic mail: zhangxc@rpi.edu.

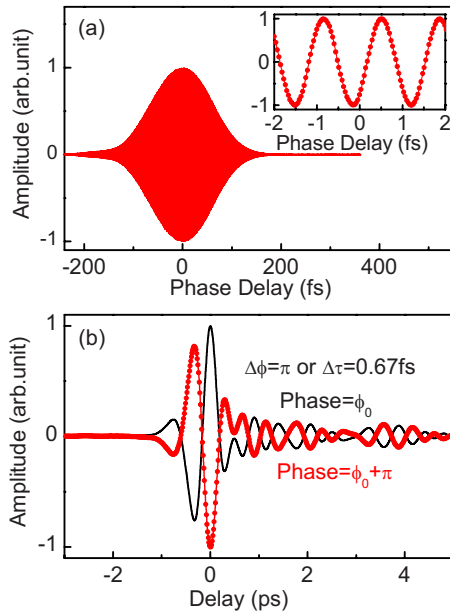


FIG. 2. (Color online) (a) Phase scan obtained by continuously changing the insertion of the fused silica wedge pair while keeping the delay line for the terahertz waveform at the peak terahertz electric field. The inset shows a zoomed-in portion of the phase scan, indicating the precise control over the relative phase between  $\omega$  and  $2\omega$  pulses. (b) Two terahertz waveforms with opposite polarities due to  $\pi$  phase shift induced by changing the relative insertion of the wedge pair in the phase compensator.

collimated and refocused by a pair of parabolic mirrors (both with an effective focal length of 4 in.) and are detected using electro-optic sampling with a 0.12 mm GaP crystal.<sup>12</sup> Figure 2(a) shows an interferometric phase scan obtained by continuously changing the insertion of one of the wedges while keeping the delay timing for the terahertz waveform scan at the peak terahertz electric field with a distance between the phase compensator and the focusing parabolic mirror less than 0.2 m (i.e., at close contact distance). With the precise control of the relative phase between the  $\omega$  and  $2\omega$  pulses, as well as the control of the polarization of the  $2\omega$  beam, a peak terahertz electric field of over 60 kV/cm can be routinely obtained in ambient air with total excitation energy of about 500  $\mu$ J. The inset of the figure shows the same phase curve in an extended scale, which indicates capability of the phase compensator for fine and stable controlling of the phase between the  $\omega$  and  $2\omega$  pulses. Figure 2(b) shows two terahertz waveforms obtained with the relative phase between  $\omega$  and  $2\omega$  beams changed by  $\pi$  (corresponding to 0.67 fs in time), respectively. Compared to previous work,<sup>11</sup> in which a piezostage in combination with a retroreflector was used to directly change the phase delay between the  $\omega$  and  $2\omega$  beams, the waveforms obtained are much more stable due to minimization of the phase fluctuation with the new phase compensator.

To quantitatively compare the performances of our current and previous phase compensators, we evaluate them in terms of both dynamic range (DR) [i.e., DR defined as the ratio between peak amplitude of the terahertz signal (waveform) and the standard deviation of the noise background in the absence of the terahertz pulse] and signal-to-noise ratio (SNR) in time domain (i.e., SNR defined as the ratio of the terahertz peak amplitude to the standard deviation of the terahertz peak amplitude). Both the DRs of the current phase compensator and the previous one are about 10 000 with a

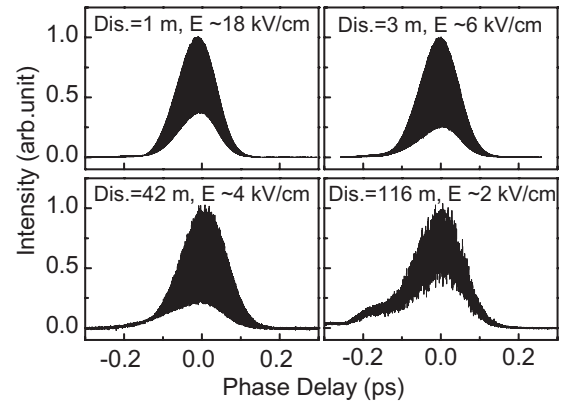


FIG. 3. Phase scan at different distances obtained by continuously changing the insertion of the fused silica wedge pair while monitoring the terahertz average power with a pyroelectric detector. The optical beams ( $\omega$  and  $2\omega$ ) are focused locally by a parabolic mirror with a focal length of 8 in. after traveling in the air at different distances.

lock-in time constant (TC) of 100 ms, indicating that the terahertz wave generation efficiencies with both compensators are very similar. However, with our current phase compensator, a SNR of about 800 can be obtained while the SNR with the previous phase compensator is no more than 100, both with a TC of 100 ms. The significant difference in SNRs is due to the better phase stability of our new approach.

To verify the feasibility of remote terahertz wave generation in ambient air with the phase compensator, terahertz signals with different distances between the phase compensator and the parabolic mirror are tested. Figure 3 plots the interferometric phase scans obtained by changing the relative phase between  $\omega$  and  $2\omega$  pulses while monitoring the emitted terahertz power with a pyroelectric detector. Each terahertz power phase curve shown in Fig. 3 shows a nonzero feature, which is unexpected from the amplitude phase curve in Fig. 2(a). This seems related to the chirp of  $\omega$  and  $2\omega$  pulses. When the prechirp of the fundamental pulse from the amplified laser system is varied by changing gratings separation in the compressor of the amplified laser, both the shape of the phase curve and the ratio between the nonzero value and the peak power can be changed significantly. Currently, we attribute the nonzero feature to the unbalanced chirp of  $\omega$  and  $2\omega$  pulses, i.e., the  $\omega$  and  $2\omega$  pulses cannot be near-chirp-free pulses simultaneously.

The terahertz waveforms and spectra (insets) shown in Figs. 4(a) and 4(b) are obtained at distances of 42 and 116 m, respectively, using 0.12 mm GaP crystal as the detector. As shown in Fig. 4(b), at a beam propagating distance of 116 m, the peak signal/noise ratio around 1.7 THz in the frequency domain is greater than 100 with a TC of 100 ms, despite the strong air turbulence existing in the experimental environment. It should be pointed out that when the optical beam propagating distance is increased to over 20 m, additional parallel glass plates have to be inserted into the 800 nm arm of the phase compensator to further compensate for the increasing temporal walkoff between  $\omega$  and  $2\omega$  pulses as the distance increases. This result verified the feasibility of remote generation of broadband intense terahertz waves using air or laser-induced air plasma as the emitting medium, which is one of the most important steps toward standoff terahertz sensing and identification.

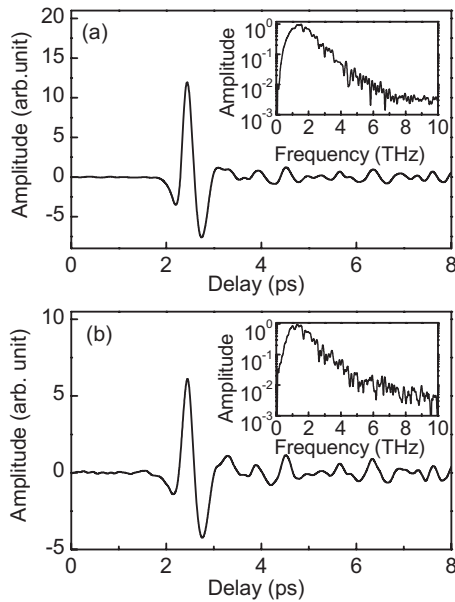


FIG. 4. Terahertz waveforms and spectra (insets) generated by sending optical beams at distances of (a) 42 m and (b) 116 m, respectively, and focusing them locally using a parabolic mirror with an effective focal length of 8 in. The peak signal/noise ratio of the spectrum is greater than 100 with a TC of 100 ms.

The phase compensator demonstrated here cannot only be used to optimize terahertz emission from laser-induced gas plasma but also can be used in coherent control of plasma formation, high harmonic generation in gas plasmas, and other physical processes with the excitation by femtosecond pulses. For some experiments where a gas cell is used,<sup>13</sup> the compensation of the temporal walkoff caused by a thick optical window of the cell and the optimization of the relative phase between  $\omega$  and  $2\omega$  pulses with the phase compensator demonstrated here are very crucial for efficient terahertz generation. Compared to other phase compensation methods, our phase compensator has advantages such as its wide phase tuning range crossing zero and better phase stability. For example, another phase compensation method with a time plate, made of either fused silica or  $\alpha$ -BBO, as demonstrated in Refs. 1 and 14, will cause lateral displacement between the  $\omega$  and  $2\omega$  beams which will significantly reduce the terahertz generation efficiency ( $\sim 20\%$  reduction in amplitude when a 0.192 mm fused silica time plate is rotating from the first optimal peak at about  $22^\circ$  to the third optimal peak at about  $48^\circ$ ) in tight focusing geometry, as has been verified in another independent experiment. The above

efficiency reduction will increase the difficulty of the optimization of the terahertz signal by changing the relative phase between  $\omega$  and  $2\omega$  beams since the phase curve is deformed when the time plate is rotating. In terms of DR, our current phase compensator has  $\sim 10\%$  higher than the time plate. Although in terms of SNR, the time plate is  $\sim 20\%$  higher than our current phase compensator due to the copropagation of  $\omega$  and  $2\omega$  beams in the case of time plate, the phase tunable range of a time plate is very limited and can hardly cover the entire phase scan, as shown in Fig. 2(a), even with a 10 mm thick fused silica plate, which will become inapplicable in terahertz wave generation from air plasma at stand-off distances.

In summary, we demonstrated the use of a phase compensator for high-efficiency terahertz wave generation from laser-induced gas plasma with attosecond phase compensation accuracy, which will find potential applications in remote terahertz generation from laser-induced gas plasma for remote sensing and identification, as well as in coherent control of some other physical processes excited by femtosecond laser pulses.

This work is partially supported by the Office of Naval Research and the National Science Foundation.

- <sup>1</sup>D. J. Cook and R. M. Hochstrasser, *Opt. Lett.* **25**, 1210 (2000).
- <sup>2</sup>M. Kress, T. Löffler, S. Eden, M. Thomson, and H. G. Roskos, *Opt. Lett.* **29**, 1120 (2004).
- <sup>3</sup>T. Bartel, P. Gaal, K. Reimann, M. Woerner, and T. Elsaesser, *Opt. Lett.* **30**, 2805 (2005).
- <sup>4</sup>M. Kreß, T. Löffler, M. D. Thomson, R. Dörner, G. Glimpel, K. Zrost, T. Ergler, R. Moshhammer, U. Morgner, J. Ullrich, and H. G. Roskos, *Nat. Phys.* **2**, 327 (2006).
- <sup>5</sup>H. Zhong, N. Karpowicz, and X.-C. Zhang, *Appl. Phys. Lett.* **88**, 261103 (2006).
- <sup>6</sup>K. Y. Kim, J. H. Glowina, A. J. Taylor, and G. Rodriguez, *Opt. Express* **15**, 4577 (2007).
- <sup>7</sup>H. G. Roskos, M. D. Thomson, M. Kreß, and T. Löffler, *Laser Photonics Rev.* **1**, 349 (2007).
- <sup>8</sup>N. Karpowicz, J. Dai, X. Lu, Y. Chen, M. Yamaguchi, H. Zhao, X.-C. Zhang, L. Zhang, C. Zhang, M. Price-Gallagher, C. Fletcher, O. Mamer, A. Lesimple, and K. Johnson, *Appl. Phys. Lett.* **92**, 011131 (2008).
- <sup>9</sup>N. Karpowicz, J. Chen, T. Tongue, and X.-C. Zhang, *Electron. Lett.* **44**, 544 (2008).
- <sup>10</sup>K. Y. Kim, A. J. Taylor, J. H. Glowina, and G. Rodriguez, *Nat. Photonics* **2**, 605 (2008).
- <sup>11</sup>X. Xie, J. Dai, and X.-C. Zhang, *Phys. Rev. Lett.* **96**, 075005 (2006).
- <sup>12</sup>Q. Wu and X.-C. Zhang, *Appl. Phys. Lett.* **67**, 3523 (1995).
- <sup>13</sup>Y. Chen, M. Yamaguchi, M. Wang, and X.-C. Zhang, *Appl. Phys. Lett.* **91**, 251116 (2007).
- <sup>14</sup>Y. Oishi, M. Kaku, A. Suda, F. Kannari, and K. Midorikawa, *Opt. Express* **14**, 7230 (2006).